

# DAMAGE ASSESSMENT OF STRESS-THERMAL CYCLED HIGH TEMPERATURE

Jaehyung Ju, Michael Prochazka, Ben Ronke, and Roger Morgan

*Polymer Technology Center  
Department of Mechanical Engineering  
Texas A&M University  
College Station, TX 77843-3123*

Eugence Shin  
*NASA Glen Research Center*

## ABSTRACT

We report on the characterization of bismaleimide and polyimide carbon fiber composite, microcrack development under stress thermal cycling loading. Such cycles range from cryogenic temperatures associated with cryogenic fuel (LN, LOX) containment to high temperatures of 300°C associated with future hypervelocity aer propulsion systems. 2/c

- Microcrack development thresholds as a function of
  - Temperature range of the thermal cycle;
  - The number of cycles;
  - The applied stress level imposed on the composite are reported.

We have conducted stress-thermal cycles on thin bismaleimide-woven carbon fiber foils for three temperature range cycles:

1. Ambient temperature  $\leftrightarrow$  -196°C
2. Ambient temperature  $\leftrightarrow$  150°C; 200°C; 250°C
3. -196°C  $\leftrightarrow$  250°C

The principle findings are that the full cycles from -196°C up to 250°C cause the most significant microcrack development. These observations indicate that the high temperature portion of the cycle under load causes fiber-matrix interface failure and subsequent exposure to higher stresses at the cryogenic, low temperature region results in composite matrix microcracking as a result of the additional stresses associate with the fiber-matrix thermal expansion mismatch.

Our initial studies for 12 ply PMR – II – 50 polyimide/M6OJB carbon fabric  $[0_f, 90_f, 90_f, 0_f, 0_f, 90_f]_s$  composites will be presented. The stress-thermal cycle test procedure for these will be described. Moisture absorption characteristics between cycles will be used to monitor interconnected microcrack development. The applied stress level will be 75% of the composite cryogenic (-196°C) ultimate strength.

**KEY WORDS:** Durability and Aging, Matrices, Polymers, Mechanical and Physical Properties

## INTRODUCTION

This paper consists of three areas namely: (i) Modeling of the electron beam curing of composites; (ii) Materials development, and (iii) Thermal-stress cycle damage mechanism characterization. The progress/accomplishments during the preceding year are as follows:

In this processing area, the time temperature profiles of electron beam cured epoxides have been modeled in terms of chemical cure parameters and correlated with experimental observations. The process window, in order to avoid moisture-induced blistering, has been developed in terms of degree of cure, resin yield stress, moisture diffusion, and vapor pressure. Also, the temperature gradient-time characteristics across the fiber-matrix interface as a function of processing parameters has been modeled [1-4].

The primary materials development issue that is being addressed is to reduce the  $\Delta T$  between the composite processing cure temperature and cryogenic service environment temperature in order to minimize composite thermal expansion mismatch stress build-up and associated microcrack development. In order to decrease  $\Delta T$ , which at present is near 500 °C, we are developing solid-state, low temperature radiation curable resins. We have developed N-vinylpyrrolidone-BMI electron beam curable resins that are 80 % reacted with a cure temperature of only 50 °C and a resulting  $T_g$  of 180 °C [5-18].

For thermal-stress cycle damage mechanism characterization we have investigated cycles that range from cryogenic temperatures associated with cryogenic fuel (LN, LOX) containment to high temperatures of 300 °C associated with future hypervelocity aeropropulsion systems. We have conducted stress-thermal cycles on thin bismaleimide-woven carbon fiber foils for three temperature range cycles:

- Ambient temperature  $\leftrightarrow$  -196 °C
- Ambient temperature  $\leftrightarrow$  -150 °C; 200 °C; 250 °C
- -196 °C  $\leftrightarrow$  250 °C

The principal findings are that the full cycles from -196 °C up to 250 °C cause the most significant microcrack development. These observations indicate that the high temperature portion of the cycle under load causes fiber-matrix interface failure and subsequent exposure to higher stresses at the cryogenic, low temperature region results in composite matrix microcracking as a result of the additional stresses associated with fiber-matrix thermal expansion mismatch [16-39].

## RESULTS AND DISCUSSION

### 1. Processing Modeling

**1.1 Background:** The objective of this current study is to develop a hygrothermal model of a thick thermoset resin during e-beam cure that can predict the temperature evolution, the glass transition temperature rise characteristics, dynamic change in the resin yield stress and water vapor pressure, and all combined effects on the influence of initiator concentrations and heat exchange with the exterior, that will guide and optimize the curing process in order to achieve:

- full and uniform resin cure
- minimum residual stress that results from the temperature gradient in the resin
- the avoidance of moisture blistering induced by the vapor pressure induced cavitation within the resin

To reach this goal, the reaction kinetics to describe the cure behavior was modeled based on the experimental data and the attempts at optimizing e-beam cure process were made. The two-dimensional model is shown in Figure 1 used in this study.

**1.2 Modeling Methodology:** Figure 2 shows the schematic representation of the modeling methodology. The modeling approach consists of three main parts. First, general heat equations together with the reaction kinetics based on the experimental data are solved simultaneously to determine degree of cure and local temperature within the sample as a function of dose.

Second, the local yield stress of the resin,  $\sigma_y$ , during cure is determined from the generic model, which is a function of  $T_g$  and temperature. Since  $T_g$  is connected to the degree of cure,  $\alpha$ , using the

phenomenological equations from the experimental curve  $T_g = f(\alpha)$ ,  $\sigma_y$  can be obtained as a function of dose.

Third, the local water vapor is compared with the local yield stress of the resin during cure to predict the threshold where the local water vapor pressure exceeds that of the polymeric cavitation resin yield stress, thus the moisture induced microvoid formation may occur (blistering) and to study corresponding conditions. It was assumed that the internal pressure of a cavity is approximately equal to the water pressure at the same conditions. The local water vapor pressure is calculated using the NBS equation of state for water and simulated temperature field at given time and dose.

Once the model is verified with experimental results of temperature variations during e-beam cure, dynamic variation of  $T_g$  and  $\sigma_y$  against  $\alpha$ , and the influence of the various processing factors on the thermal-time characteristics is investigated to guide and optimize the e-beam cure process. The resin thermal-time profile is fed-back into the e-beam dose-time sequences for a specified geometry, such that moisture vapor pressure induced permanent blister formations are avoided.

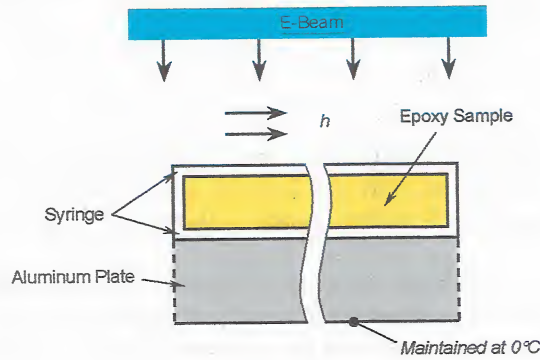


**Figure 1.** Schematic diagrams of the two-dimensional model.

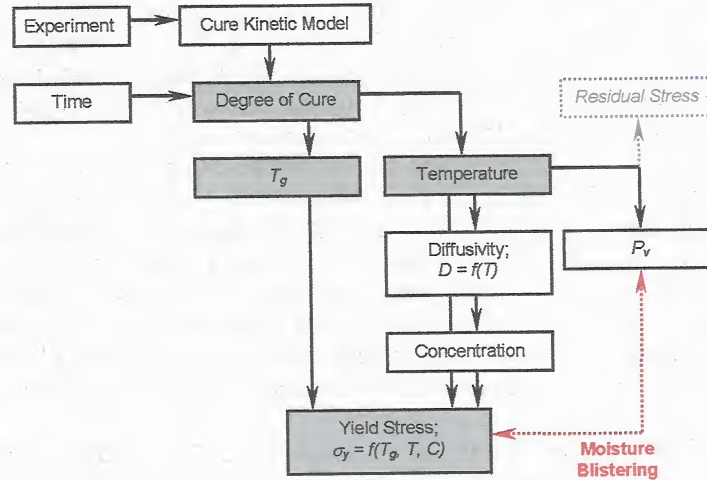


**Figure 2.** Schematic representation of hygrothermal modeling methodology.

**1.3 Principal Findings:** The hygrothermal model has been developed to predict the temperature evolution, epoxy conversion ratio,  $T_g$  increase and associated resin yield stress rise, absorbed moisture

vapor pressures in  $I^+SbF_6^-$  catalyzed DGEBA epoxy cationic polymerized resin systems during e-beam induced polymerization and the effects of four different initiator concentrations: 0.1, 1, 3, and 10 phr. An autocatalytic model was chosen to describe the cure kinetics for this study by treating the reaction constants as adjustable parameters based on measured temperature data during e-beam treatment and provided excellent agreement with experimental results.

The numerical results showed that the cure reaction of  $I^+SbF_6^-$ - DGEBA epoxy resin is diffusion controlled, but long lived reactive species allowed for measurable increase in conversion after e-beam irradiation (post cure effects). Higher initiator concentration results in higher degree of cure at a dose and higher temperature rise, resulting in more significant temperature and conversion ratio gradients within the sample under given experimental conditions.

One simulation was performed to optimize the e-beam cure process by controlling the thermal history of the sample via adjusting thermal boundary conditions. The results showed that the temperature gradient in the resin could be reduced significantly and the critical condition could be avoided during cure, while obtaining the same degree of cure as before.

## 2. Materials Development

**2.1 Background:** Bismaleimide (BMI) resins have shown great potential for space applications because of their ability to bridge the thermal stability gap between epoxy and high temperature polyimide resins. Also, BMI has many advantages such as low moisture absorption, low cost, nonvolatility and ease of processing.

Thermal cure kinetics and related resin modification together with properties and structure characterization of BMI systems have already been widely studied [5-14]. However, conventional thermal fabrication has many limitations, such as long curing time, thermal expansion fiber matrix mismatch induced stress, cure induced shrinkage and associated microcrack, expensive tooling, hazardous chemical volatiles and size limitation for autoclave. Therefore, interest in electron beam (E-beam) curing of polymer matrix composites over the last few years has dramatically increased due to its favorable advantages compared to thermal curing method such as reduced curing time, lower cooling cost, shelf stable resin systems, low health risks and curing at selectable temperatures. Moreover, E-beam curing offers the potential to fabricate large integrated structures for space transportation systems, thus eliminating the need for expensive autoclave processing, which also has size limitations to process such large structures. In addition, E-beam processing could potentially fabricate unique composite hybrids that could not be produced by conventional thermal fabrication processes.

However, since the reports that BMI resins could not be cured by E-beam radiation [15], there are only few papers on studies of E-beam curing of BMI systems. Generally, reactive diluents were used as the solvent to decrease the viscosity of BMI resins, which would favor the diffusion of molecules, thus increasing the reactivity of BMI systems. It has been shown that N-vinylpyrrolidone (NVP) is a suitable reactive diluent in BMI systems because it has a similar structural unit to BMI, and the crosslinked polymers could achieve good thermal and mechanical properties. Marie-Florence G. -L. et al. [15] reported that the percentages of residual maleimide functions in their BMI/NVP systems are less than 10 % and the  $T_g$  of the related products are around 240 °C after 400 kGy dosage E-beam curing at 50 kGy per pass.

It is known that E-beam radiation will raise the temperature of the samples. The temperature rise,  $\Delta T$ , in the samples during E-beam radiation is proportional to the exposure dosage  $D$  and material specific heat capacity  $C_p$ :  $\Delta T = D / C_p$ . Since the temperature factor plays a critical role on cure kinetics, cure mechanism, processing and the performance of final products, the studies of related temperature rise during E-beam curing are very important. Unfortunately, there are no data on the temperature issue of E-beam curing of BMI systems.



In this study we undertook a basic study on E-beam curing of modified BMI resin with temperature monitoring in order to investigate the relationships of temperature rises, dosage and dose rate and related cure extents. This will help us understand the involved reactions and mechanisms and to control the processing and performance of final products more easily.

**2.2 Principal Findings:** Low intensity E-beam such as 10 kGy and 20 kGy per pass exposure cannot initiate the polymerization of 4,4'-Bismaleimidodiphenylmethane / BMI-1,3-tolyl / o,o'-diallylbisphenol A BMI system. Higher intensity E-beam exposure at the dose rate of 40 kGy per pass can achieve high reaction conversion of BMI of 75 % (Figure 3). However, the temperature of BMI reaches up to 250 °C, which induces the thermally cure mechanism (Figure 4).

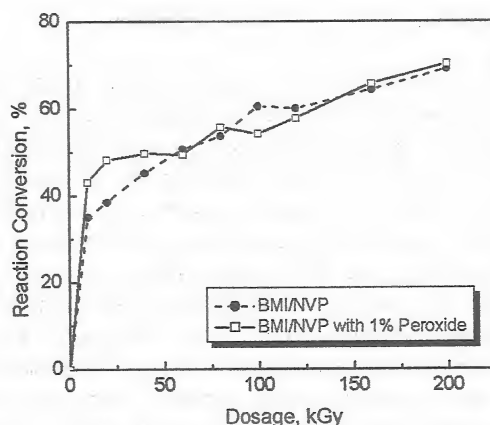


**Figure 3.** The reaction conversion of BMI/NVP with and without initiator vs E-beam dosage from FT-IR measurement (690cm<sup>-1</sup>); Dose rate: 10 kGy per pass.

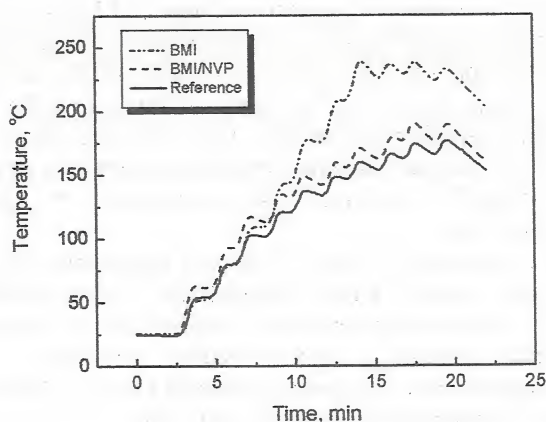


**Figure 4.** Temperature data of BNI and BMI/NVP during E-beam curing at the rate of 40 kGy per pass (total 400 kGy dosage).

Block radius R=38.0mm (Maximum strain = 0.43%)				
No. of Cycles	Heating Rate is 0.72 °C/min		Heating Rate is 3.42 °C/min	
	Tension	Compression	Tension	Compression
2	0.06	0	0.12	0
4	0.06	0	0.15	0
6	0.08	0	0.22	0.01
8	0.08	0.02	0.46	0.06

**Table 4.** Number of Microcracks for different moisture conditions at temperature range of  $-196^{\circ}\text{C}$  to  $250^{\circ}\text{C}$

Air Conditions	Block radius, R=38.0mm (Maximum strain = 0.43%)	
	Tension	Compression
Dry	0.11	0.01
Moist	0.17	0.03

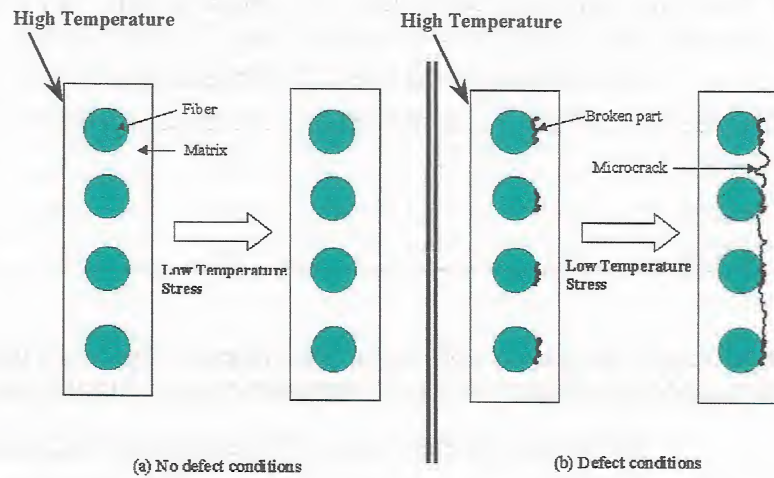


**Figure 5.** Failure procedure of initial transverse microcracks.

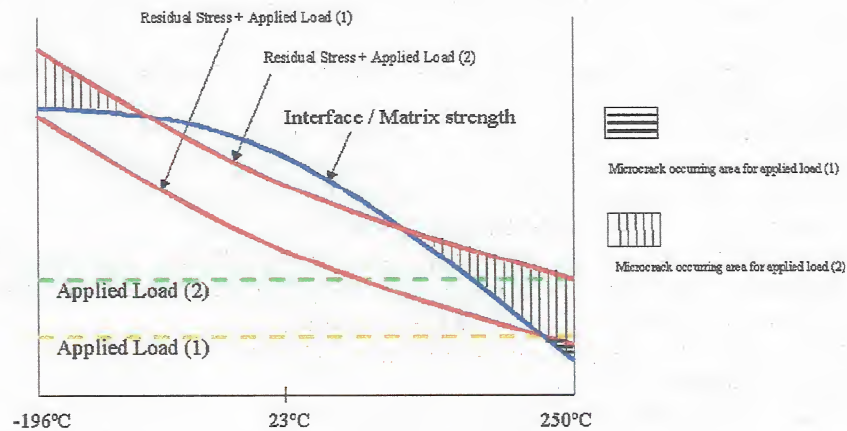


Figure 6. Microfailure regions at different loading conditions.

### ACKNOWLEDGEMENTS

The authors thank the Air Force Office of Scientific Research sponsored by Dr. Charles Lee, NASA-Glen, and the Advanced Project Research program of the State of Texas for financial support and encouragement of these studies.

### REFERENCES

1. L. Bonnaud, R. Rahul, J. Choi, V. Lopata, J. Lu, and R. J. Morgan, to be submitted to *Journal of Composite Materials*, (2003).
2. S. W. Moon, R. J. Morgan, and S. C. Lau, submitted to *Journal of Composite Materials*. (2003a).
3. S. W. Moon, R. J. Morgan, and S. C. Lau, submitted to *Journal of Composite Materials*. (2003b).
4. Q. Zheng and R. J. Morgan, *Journal of Composite Materials*, 27 (15), 1468, (1993).
5. J. Mijović and S. Andjelić, *Macromolecules*, 29 (1), 239, (1996).
6. T. M. Donnellan and D. Roylance, *Polymer Engineering and Science*, 32 (6), 409, (1992).
7. M. Suzuki, et al., *Journal of Applied Polymer Science*, 44, 1807, (1992).
8. A. Seris, et al., *Journal of Applied Polymer Science*, 48, 257, (1993).
9. A. T. Tungare and G. C. Martin, *Polymer Engineering and Science*, 33 (10), 614, (1993).
10. R. J. Morgan, et al., *Polymer*, 34 (4), 835, (1993).
11. M. Grenier-Loustalot and L. D. Cunha, *Polymer*, 38 (26), 6303, (1997).
12. R. J. Morgan, et al., *Polymer*, 38 (3), 639, (1997).
13. J. C. Phelan and C. S. P. Sung, *Macromolecules*, 30 (22), 6837, (1997).
14. J. C. Phelan and C. S. P. Sung, *Macromolecules*, 30 (22), 6845, (1997).
15. M. Grenier-Loustalot, V. Denizot, and D. Beziers, *High Performance polymers*, 1, 181, (1995).
16. D. Amatore, *NASA Office of Aeronautics and Space Transportation Technology*, 6 (2), 13, March/April, (1988).
17. R. J. Morgan, D. Li, J. Lu, S. Moon, R. Ribeiro, *SAMPE International Symposium*, 47, 585 (2002).
18. A. Paillous and C. Pailler, *Composite*, 25 (4), 287, (1994).
19. J. A. Narin, *Journal of Composite Materials*, 23, 1106, (1989).
20. H. Fukunga and T. Chou, *Journal of Composite materials*, 18, 339, (1984).
21. E.E Shin, R. J. Morgan, J. Zhou, *Proceedings of Advanced High Temperature Engine Materials Technology Project*, Volume 1, High Temp. NASA/CP-1999-208915, Paper 13, (1999).

22. E.E. Shin, R. J. Morgan, J. Zhou, J. K. Sutter and M.A. Meador, *SAMPE International Symposium*, 44, 2382 (1999).
23. T. Shimokawa, H. Katoh, Y. Hamaguchi, S. Sanfongi, and H. Mizuno, *Journal of Composite Materials*, 36 (7), 885, (2002).
24. K.Noda, A.Takahara and T.Kajiyama, *Polymer*, 42, 5803, (2001).
25. Y. Li, X. Tand, J. A. Miranda, H. Sue, and J. D. Witcomb, *Proceedings of the American Society for Composite*, 15<sup>th</sup> Annual Technical Conference, 558 (2000).
26. C.Li, Ph. D. Dissertation at Texas A&M University, (2001).
27. N. Sato, T. Kurauchi, S. Sato, O. Kamigaito, *Journal of Materials Science*, 19, 1145, (1984).
28. N. Sato, T. Kurauchi, S. Sato, and O. Kamigaito, *Journal of Materials Science*, 26, 3891, (1991).
29. J. A. Nairn, *Journal of Composite Materials*, 23, 1107, (1989).
30. J. Renard, J. P. Favre, and T. Jeggy, *Composite Science and Technology*, 46, 29, (1993).
31. L. N. McCartney, *Composites*, 24 (2), 84, (1993).
32. H. T. Hahn, *Journal of Composite Materials*, 10, 266, (1976).
33. K. Chaoui, A. Chudnovsky, and A. Moet, *Journal of Materials Science*, 22, 3873, (1987).
34. C. Henaff-Gardin, M. C. Lefarie-Frenot, and D. Gamby, *Composite Structure*, 36, 131, (1996).
35. P. W. M. Peters and S. I. Andersen, *Journal of Composite Materials*, 23, 944, (1989).
36. L.T. Drzal, M. J. Rich, and M. F. Koenig, *Journal of Adhesion*, 18, 49, (1985).
37. S. Kessler, H. McManus, and T. Matuszeski, *Proceedings of the American Society for Composites*, September, Blacksburg, VA, (2001).
38. D.W. Sohn, Q. Zhou, and N. -H. Sung, *Proceeding of the 52<sup>nd</sup> Annual Technical Conference on Plastics Engineering*, 2, 2382, (1994).
39. D. A. Biro, G. Plezier, and Y. Deslandes, *Composite Science and Technology*, 46, 293, (1993).